As originally published in the IPC APEX EXPO Conference Proceedings.

Drop Test Performance of A Medium Complexity Lead-Free Board After Assembly and Rework

P. Snugovsky, J. Bragg, E. Kosiba, M. Thomson, B. Lee, R. Brush, S. Subramaniam, M. Romansky
Celestica International Inc.

A. Ganster*, W. Russell#, J. P. Tucker**, C. A. Handwerker**, D. D. Fritz##
*Crane Division NSWC, #Raytheon, **Purdue University, ##SAIC

Abstract
The mechanical behavior of printed circuit assemblies (PCA) at high strain rates is very important for the reliability of products used in harsh environments. The transition to Pb-free materials in the general electronics industry significantly impacts the mechanical reliability of solder joint interconnects, as widely recognized by the consumer electronics industry. Numerous mechanical behavior studies using a drop test have been reported on ball grid array components with different Pb-free solders. This study is focused on leaded and leadless components in comparison with ball grid array components assembled with Pb-free solder on medium complexity boards. This study is part of a large scale NASA DoD project and utilized the same board design, assembly, and rework processes of that larger project. Components were attached to the boards using Pb-free solder SAC305. The TSOP-50, TQFP-144, QFN-20, and CLCC-20 components were then hand reworked using conventional SnPb solder to address the sustainment issue. Both 1x and 2x reworks were performed on the non-BGA devices. The PDIP components were also reworked; however, their analysis is not covered in this paper.

In the present work, a board-level drop shock test was performed on nine assemblies, each with 63 components attached. Each board was monitored for shock response and net electrical resistance for all components. In addition, three of these cards were monitored for board surface strain. The assemblies were fixtured to a drop table 3-up and subjected to either 340G or 500G shocks, for a total of 20 drops per board. The shock response, net resistance and strain were recorded in-situ during each drop. The vast majority of the electrical failures occurred on the PBGAs, which were not reworked in this study. Only three of the leaded and leadless components experienced electrical failure.

Damage from the drop shock test was assessed by examining electrically failed and non-failed non-BGA parts by dye-and-pry and cross-section analyses followed by microstructural examination and defect mapping. It was found that the predominant failure mechanism was board side pad cratering. The cracks propagated through the board material between the laminate and glass fiber under the pad. Electrical failure was only observed when the Cu trace was broken. Of the leaded components that were electrically functional after drop testing, approximately one third were found to be mechanically damaged with pad cratering after dye and pry inspection. This hidden damage may be a reliability concern depending on the field use conditions. Only three leaded components electrically failed, two that were reworked with SnPb solder and one that was not reworked and contained the original SAC 305 solder. Of the two reworked joints that failed electrically, only the TQFP-144, the more compliant leaded component, showed signs of SnPb solder joint fatigue fracture. The failure of the other two components was due to pad cratering and severed traces. There was no correlation found between the number of reworks and the amount of electrical or mechanical failure since only three non-BGA components failed in the test. Most importantly, this sample set showed no difference in drop test performance between SnPb-reworked and non-reworked Pb-free solder joints for non-BGA components. More data will be available upon completion of the NASA DoD Pb-free project.

Introduction

Impact due to drop/shock has recently become more important in the reliability of microelectronics. [1] There are a number of causes for this transition. First, greater functionality in circuit cards necessitates an increase in the density of components with a corresponding decrease in pitch size. These smaller solder joints experience higher strain rates under drop/shock, and are more prone to fracture. Second, concurrent to the decrease in pitch size, the consumer market has shifted from SnPb eutectic solder to Pb-free solders due to environmental legislation. Lead-free solders are less compliant than SnPb, and so they absorb a smaller fraction of the impact energy. Numerous mechanical behavior studies using drop tests have been reported on ball grid array components with different Pb-free solder materials using drop test. In particular, Suh et. al. [1] found that SAC 105 exhibited a performance ten times better than SAC 405 in drop testing when designating 5% increase in resistance as the onset of failure. Since no apparent difference could be observed in the intermetallic layer or interfacial morphology, the authors proposed that the bulk solder behavior affected the fracture behavior of the solder joints by applying a concept called extrinsic toughening. SAC 105 is more compliant and deformable than SAC 405, so less energy is available to propagate a crack in SAC105 joints.

While the effects of Pb-free solder alloy on drop/shock performance have been studied, much less is known about the effect of reworked joints. In harsh environment applications such as military or aerospace, reliability is critical, and drop impact becomes a more significant concern. This paper reports on the findings of a joint study between Celestica Inc., Crane Division NSWC, Raytheon, Purdue University, and SAIC on how the drop shock performance of Pb-free leaded and leadless solder joints is affected by reworking the joints with SnPb eutectic solder. Rework of legacy electronics in military and aerospace systems will necessitate the continued use of SnPb solder for rework for decades. The question this study was focused on answering is whether SnPb eutectic solder could be used to rework Pb-free solder joints without degrading drop shock performance of the resulting components. If no degradation occurs, only SnPb solder will be required for rework.
This work is part of the larger scale NASA DoD project and utilized the same medium complexity board design, assembly, and rework processes of that larger project. Similar rework studies are being performed for vibration and thermal cycling environments.

Experimental -Test Vehicle
The test vehicle used for this study, shown in Figure 1, was designed by the Joint Group on Pollution Prevention (JG-PP), the National Aerospace Agency (NASA) and the Department of Defense (DoD) consortia to meet IPC-6012, Class 3 requirements. The 6-layer board with 0.5-ounce copper layers was 368.3mm x 228.6mm x 2.29mm in size. An FR-4 laminate was used as per IPC-4101/26 with a minimum T_g of 170°C. The surface finish of the boards was Immersion Ag (ImmAg). The boards were populated with components representative of the parts used for military and aerospace systems. A variety of surface mount technology (SMT) and plated through-hole (PTH) components were daisy chained for electrical monitoring during testing by an event detector. The components monitored during drop testing are shown in Table 1.

Figure 1: Drop Test Vehicle

Table 1: Component Selection

Package	Ball or Finish	Dimensions (mm x mm)	Pitch (mm)	TV-Drop
PBGA225	SAC405	27 x 27	1.5	U02, U04, U04, U06, U18, U21, U43, U44, U55, U56
CSP100	SAC 105	10 x 10	0.8	U19, U32, U33, U35, U36, U37, U42, U50, U60, U63
TQFP-144	Matte Sn	20 x 20	0.5	U01, U03, U07, U20, U31, U34, U41, U48, U57, U58
TSOP-50	Sn	10.16 x 20.95	0.8	U12, U25, U29, U39, U61
	SnBi	10.16 x 20.95	0.8	U16, U24, U26, U40, U62
PDIP-20	NiPdAu	7.5 x 26.16	2.54	U8, U23, U49
	Sn	7.5 x 26.16	2.54	U11, U30, U38, U51, U59
CLCC-20	SAC305	9 x 9	0.8	U09, U10, U13, U14, U17, U22, U45, U46, U52, U53
QFN	Matte Sn	5 x 5	0.65	U15, U27, U28, U47, U54

Experimental - Assembly

Nine test vehicles for the Crane rework study were assembled at the BAE Systems, Irving Texas facility. The Sn3.0Ag0.5Cu (SAC305) solder was chosen for SMT assembly using a conventional reflow profile for SAC305. Then the PTH components were inserted and attached at the TT Apsco Painesville, Ohio facility using Sn0.7Cu0.5Ni (≤0.01Ge) (Sn100C) solder. The wave pot temperature was 265°C. Following initial assembly, selected TSOP-50, TQFP-144, QFN-20, and CLCC-20 components were then hand reworked using conventional SnPb (63/37) solder to address the sustainment issue. Both 1x and 2x hand reworks were performed using new components.

Experimental – Rework Plan

The rework plan was designed to maximize the number of relevant comparisons of 0X, 1X and 2X rework while preserving enough data points for meaningful statistical analysis. In a drop test, board deflection (and thus solder joint strain) will vary based on the location of the component. Comparisons of like components from different locations on the board can be made, but it must be assumed that the variance in deflection across the board is negligible. Ideally comparisons are made among components of the same solder alloy, surface finish, and location on the board, with the only difference being the number of reworks. With nine boards, components were reworked in either a 0X-1X or 1X-2X pattern. For a 0X-1X pattern, this allowed five 0X components and four 1X components for comparison, or vice versa. A similar pattern was used for the 1X-2X pattern. Other groups of 9 components/locations, for example, U24 or U12, were left in the as-assembled for future comparison with results from the remainder of NASA-DOD boards. The complete rework plan is shown in Table 2.

Table 2: Rework pattern of Drop Test Boards

Component Location	Part/Solder Alloy	Number of Reworks								
		Test Board Number								
		#1	#2	#3	#4	#5	#6	#7	#8	#9
U16	TSOP 50/SnBi	1	2	1	2	1	2	1	2	1
U24	TSOP 50/SnBi	0	0	0	0	0	0	0	0	0
U26	TSOP 50/SnBi	1	0	1	0	1	0	1	0	1
U40	TSOP 50/SnBi	2	1	2	1	2	1	2	1	2
U62	TSOP 50/SnBi	0	1	0	1	0	1	0	1	0
U12	TSOP 50/Sn	0	0	0	0	0	0	0	0	0
U25	TSOP 50/Sn	1	2	1	2	1	2	1	2	1
U29	TSOP 50/Sn	2	1	2	1	2	1	2	1	2
U39	TSOP 50/Sn	1	0	1	0	1	0	1	0	1
U61	TSOP 50/Sn	0	1	0	1	0	1	0	1	0
U9	CLCC-SAC305	1	2	1	2	1	2	1	2	1
U10	CLCC-SAC305	2	1	2	1	2	1	2	1	2
U13	CLCC-SAC305	0	0	0	0	0	0	0	0	0
U14	CLCC-SAC305	0	0	0	0	0	0	0	0	0
U17	CLCC-SAC305	1	2	1	2	1	2	1	2	1
U22	CLCC-SAC305	2	1	2	1	2	1	2	1	2
U45	CLCC-SAC305	1	0	1	0	1	0	1	0	1
U46	CLCC-SAC305	0	1	0	1	0	1	0	1	0
U52	CLCC-SAC305	1	0	1	0	1	0	1	0	1
U53	CLCC-SAC305	0	1	0	1	0	1	0	1	0
U1	TQFP-144/Sn	1	2	1	2	1	2	1	2	1
U3	TQFP-144/Sn	0	0	0	0	0	0	0	0	0
U7	TQFP-144/Sn	2	1	2	1	2	1	2	1	2
U20	TQFP-144/Sn	0	0	0	0	0	0	0	0	0
U31	TQFP-144/Sn	1	2	1	2	1	2	1	2	1
U34	TQFP-144/Sn	2	1	2	1	2	1	2	1	2
U41	TQFP-144/Sn	1	0	1	0	1	0	1	0	1
U48	TQFP-144/Sn	0	1	0	1	0	1	0	1	0

U57	TQFP-144/Sn	1	0	1	0	1	0	1	0	1
U58	TQFP-144/Sn	0	1	0	1	0	1	0	1	0
U08	PDIP-20/NiPdAu	1	2	1	2	1	2	1	2	1
U49	PDIP-20/NiPdAu	2	1	2	1	2	1	2	1	2
U23	PDIP-20/NiPdAu	0	1	0	1	0	1	0	1	0
U30	PDIP-20/Sn	2	1	2	1	2	1	2	1	2
U38	PDIP-20/Sn	1	2	1	2	1	2	1	2	1
U11	PDIP-20/Sn	0	1	0	1	0	1	0	1	0
U51	PDIP-20/Sn	1	0	1	0	1	0	1	0	1
U59	PDIP-20/Sn	0	1	0	1	0	1	0	1	0
U15	QFN/Sn	1	2	1	2	1	2	1	2	1
U27	QFN/Sn	2	1	2	1	2	1	2	1	2
U28	QFN/Sn	1	2	1	2	1	2	1	2	1
U47	QFN/Sn	1	0	1	0	1	0	1	0	1
U54	QFN/Sn	0	1	0	1	0	1	0	1	0

Experimental – Rework Processes

The Crane/NSWC rework team performed conductive rework of TSOP-50, PQFP-144, CLCC-20, and PDIP-20 component types. Convective rework was performed on the QFN-20 devices. Conductive processes were per IPC-7711 and included wicking, vacuum extraction, heat and lift, and drag soldering techniques. Component types were reworked in random order, but adjacent components requiring rework were reworked in pairs. Bottom side rework preheat of 100° C was used for all conductive rework.

Component types were reworked as follows:

- PQFP-144//TSOP-50 component leads were wicked of bulk solder with solder wick and a soldering iron. Component leads were then reheated and leads were lifted with a dental pick. Residual solder was wicked with solder wick and a solder iron. Land areas were cleaned with a solvent and brush. New parts were placed, fluxed, and soldered using multipoint drag soldering techniques. Components were cleaned with solvent and brush and inspected per J-STD-001 Class 3 requirements. Desoldering therefore required three heat cycles followed by soldering of the new part with one heat cycle. The soldering iron temperature was 640°F.
- CLCC-20 components were removed using the Solder Wrap procedure (IPC-7711) consisting of wrapping 0.036 wire solder around the component periphery and desoldering with a box tip. The component lands were cleaned of residual solder with solder wick and a soldering iron. Component castellations were bumped with solder, placed and soldered using multipoint drag soldering techniques. The component sites were cleaned after component removal and replacement and inspected per J-STD-001 Class 3 requirements. Desoldering required two heat cycles followed by soldering of the new part with one hear cycle. The soldering iron temperature was 640°F.
- PDIP-20 component leads were lightly fluxed and desoldered using a vacuum extraction process at 800°F. Upon component removal, PTH's were filled with SnPb solder and the solder was extracted. New parts were installed, fluxed, and soldered using point-to-point soldering techniques at 750°F. Component sites were cleaned with solvent and brush after component removal and replacement.
- QFN-20 components were reworked by Best, Inc., Rolling Meadows, IL.

Experimental - Drop Test

The drop test is used to determine the resistance of board level interconnects to board strain. Boards tested using this method typically fail either as interfacial fractures in the solder joint (most common with ENIG) or as pad cratering in the component substrate and/or board laminate. Outside of laboratory testing, these failure modes commonly occur during manufacturing, electrical testing (e.g. in-circuit test), card handling and field installation and use. The root causes of these types of failures are typically a combination of excessive applied strain due to process issues and/or weak interconnects due to SMT process issues and/or the quality of incoming components and/or boards. This board-level drop test is based on the JEDEC Standard JESD22-B110A known as Subassembly Mechanical Shock, as well as insight gained by Celestica after performing numerous drop tests on various internal test vehicles over the past 5 years.[2-4]

The drop test process can identify design, process, and raw materials related problems in a much shorter time frame than other development tests. In this project, the drop test was used to determine the operation and strain endurance limits of the solder alloys and interconnects by subjecting the test vehicles to accelerated environments. Unique to this test was the comparison between the interconnect robustness of as-assembled Pb-free leaded components to Pb-free leaded components reworked with SnPb solder. The limits identified in drop testing were used to compare performance differences in the Pb-free test alloy and mixed solder joints vs. the baseline standard SnPb alloy joints. The primary accelerated environments were strain and strain rate.

In this study, a board-level drop shock test was performed on nine assemblies based on the JEDEC test method JESD22-B110A. The only deviation from the JEDEC test was the layout of the test vehicle (see Figure 1). Since the test vehicle was also being used to evaluate many different component types in thermal cycling and vibration tests it did not follow the standard JEDEC layout. Each board was however monitored for shock response and for net electrical resistance for all 63 components using an event detector.

In addition, three of the cards were monitored for surface strain during the drop test. Three cards were dropped with strain monitoring in addition to the shock and resistance monitoring. Four rosette strain gauges were attached to each board at the strain gauge locations shown in Figure 2. Each strain gauge had 3 channels and the principal strain was calculated by using the strain reading from these channels.

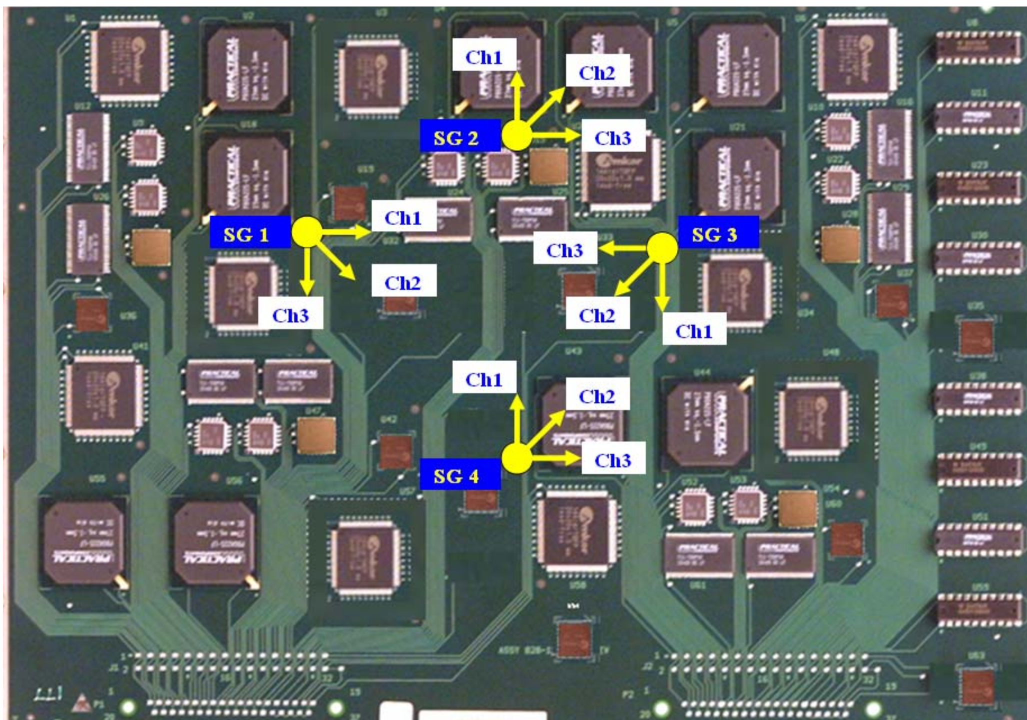

Figure 2: Test Vehicle with Strain Gages, location and orientation illustrated

Three assemblies were fixtured to the drop table at a time with the components facing down and subjected to either 340G or 500G shocks for a total of 20 drops per board (see Figure 3). The shock response, resistance and strains were recorded in-situ during each drop. A daisy-chain resistance increase greater than 300 ohm from the baseline was considered a failure. Three hundred ohms was chosen based on previous NASA DoD / JG-PP projects. The acceptance criterion was for the reworked cells to have a higher than or an equal number of drops until failure as the Pb-free components.

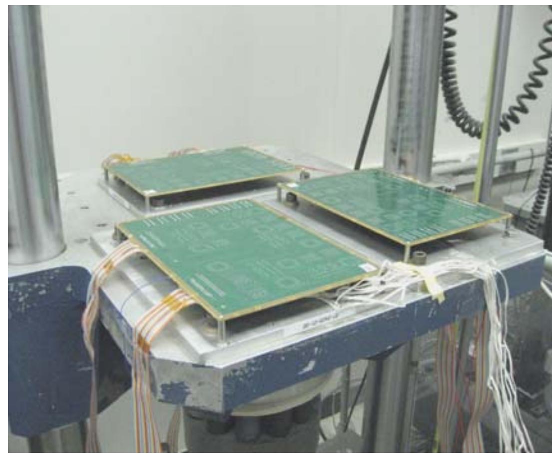

Figure 3: Test Vehicles Mounted on Drop Table

Experimental - Failure Analysis

After the drop testing was complete, eight boards were selected for destructive failure analysis. Both dye-and-pry and cross sectioning were performed, each of which was designed to determine the location, mode and mechanism of the failure. The samples selected for dye-and-pry were examined using an optical microscope after the parts were pried from the board and the results were further mapped. The cross sectioned samples were examined using optical and scanning electron microscopy (SEM) as well as analyzed by energy dispersive x-ray (EDX). The focus was to compare the quality of the solder joints of components that were reworked once using SnPb solder (therefore consisting of a mixed metallurgy of Pb and Pb-free solder), those that were reworked twice using SnPb solder (consisting of leaded solder), and those which were not reworked at all- therefore Pb-free. Only non-BGA components are described in detail in this paper.

The samples selected for destructive failure analysis represented both electrical failures (as determined through resistance monitoring of the components) as well as parts that survived the drop testing with no change to the electrical properties. In total 23 samples were dye-and-pried and 15 were cross sectioned.

Results and Discussion

Drop Test Results

After each drop, the in-situ resistance data were reviewed and each suspect net was manually checked for a high resistance and the data were recorded. The vast majority of the electrical failures occurred on the PBGAs, none of which were reworked. Out of the 90 PBGAs tested, all but one failed within 20 drops (see Table 3). In addition, all 90 CSP samples passed the electrical monitoring during drop testing. **Error! Reference source not found.** shows the physical location of the electrically failing non-BGA components.

S

Table 3: Record of Drops to Electrical Failure for PBGA-225

	82	80	87	86	85	84	83	81	60
U18	12	17	15	10	2	6	9	17	Survive
U56	14	11	13	7	9	8	16	7	14
U55	19	11	19	7	6	3	9	6	15
U2	4	11	14	4	6	4	5	15	17
U4	10	11	6	3	2	4	2	9	6
U43	11	11	6	3	5	6	7	5	8
U21	8	8	10	5	5	3	5	4	5
U44	13	12	10	10	9	7	12	11	16
U5	5	7	5	4	3	2	5	4	4
U6	7	7	5	4	2	2	5	3	3

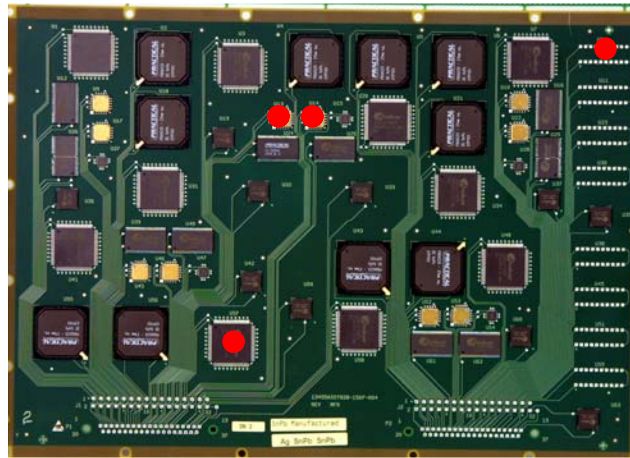

Figure 4: Location of Non-BGA Component Resistance Failures

Although 477 non-PBGA components were drop tested, only 4 had any increase in net resistance after 20 drops (see Figure 4). The 4 non-PBGA components with electrical failure had the following rework histories:

- Board SN 84, CLCC-20, U14 was **not** reworked
- Board SN 85, TQFP 144, U57 **was** reworked **once**
- Board SN 85, PDIP-20, U8 **was** reworked **once**
- Board SN 86, QFN-20, U15 **was** reworked **twice**

Since none of the PBGAs were reworked in this study and the test resulted in a small number of non-BGA electrical failures, the authors are unable to determine the comparative strength of Pb-free vs. SnPb reworked samples. However, the test does allow the conclusion that the reworked components were in general no worse than the original Pb-free components under these stress conditions and met the strain requirements of the authors.

Solder Joint Microstructure Characterization

Microstructure characterization was carried out on three different components TQFP-144, TSOP-50, and QFN-20, each in an as-assembled, 1X rework, and 2X rework condition.

Figure 5 shows the microstructure of Pb-free joints before rework. The joints consist of highly branched primary-like Sn dendrites, and Ag_3Sn+Cu_6Sn_5+Sn eutectic in interdendritic spaces and between the Sn dendrite arms. Both primary Ag_3Sn platelets and Cu_6Sn_5 were identified by EDX in the TQFP-144 solder joints. Relatively small Ag_3Sn platelets were attached to the pad intermetallic layer. No Ag_3Sn primary platelets were detected in the TSOP-50 solder joints. The primary intermetallic particles in these joints were Cu_6Sn_5 type that contained about 2% Ni and in some cases about 1% Fe. The sources of the Ni and Fe atoms were the Ni barrier layer and the Alloy 42 lead-frame material of the TSOP-50 components. The intermetallic formed between the Cu pads and solder in TQFP-144 and TSOP-50 was rather thin, 1.8 to 2.9 microns, and was of the Cu_6Sn_5 type.

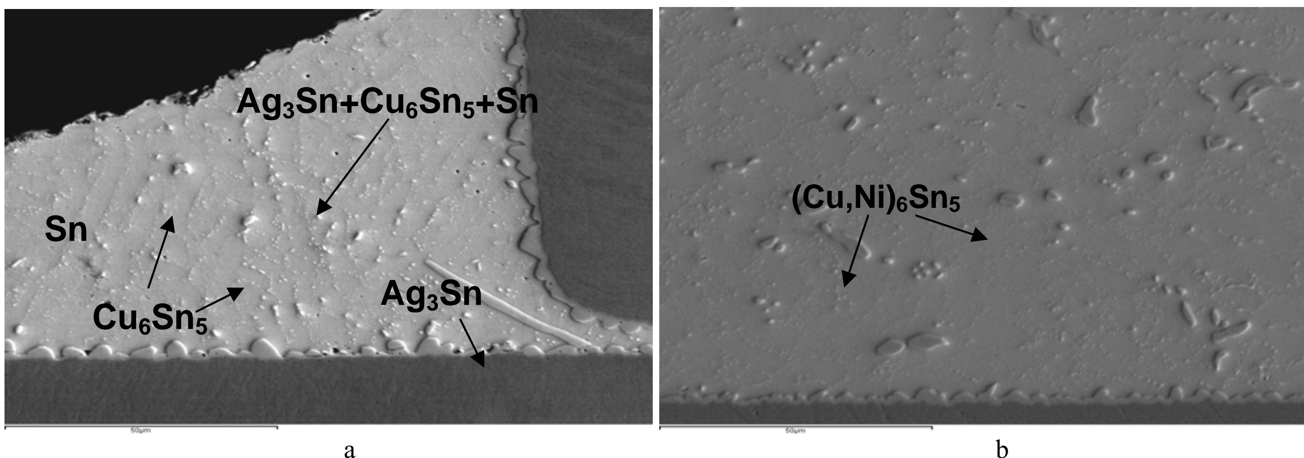

Figure 5: Typical microstructure of SAC305 solder joints before rework, SEM 1000x: a-TQFP-144; b-TSOP-50

The Pb-free leaded components were reworked with SnPb solder. As expected, the SnPb microstructures of all reworked joints were quite different from that of the as-assembled Pb-free parts. After 1X rework the joints had a SnPb eutectic structure with some primary intermetallic crystals (Figure 6). EDX analysis showed that these intermetallic particles were of the Cu_6Sn_5 type. Some joints also contained some Ni, particularly in the TSOP-50. The number of the primary intermetallic crystals was lower in the QFP-20 reworked joints than in the TQFP-144 and TSOP-50.

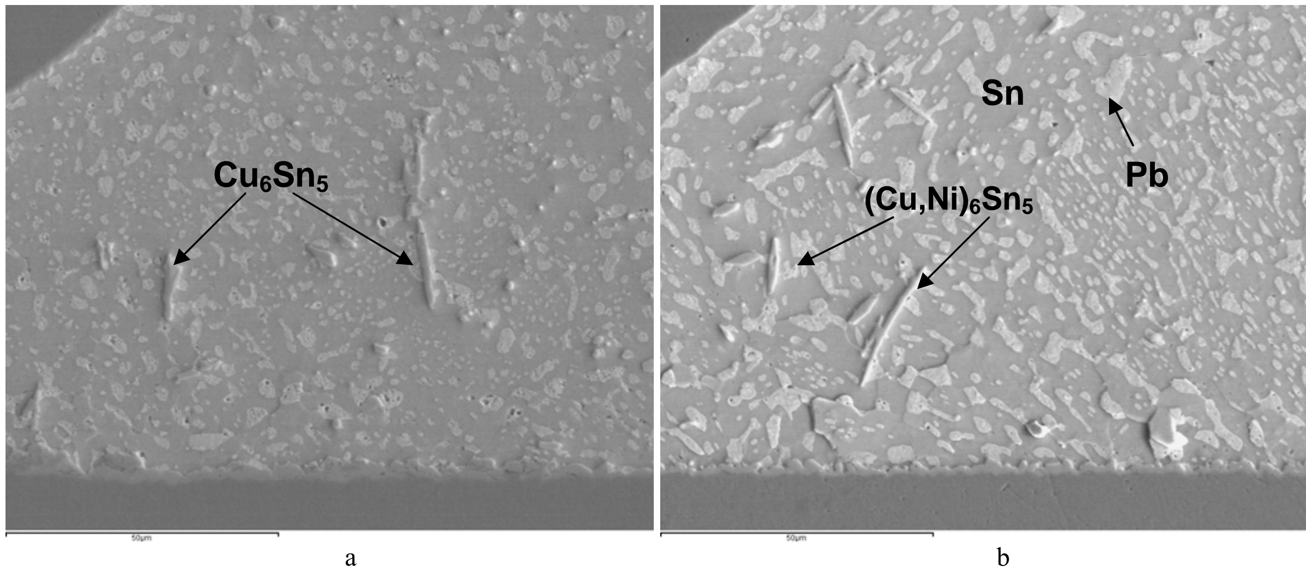

Figure 6: Typical microstructure of 1X reworked solder joints using SnPb solder, SEM, 1000X: a – TQFP-144; b – TSOP-50

A significant portion of primary intermetallic solidifies first, followed by the SnPb eutectic and depends on the primary SAC305 alloy composition. The reason for such a significant shift in composition was found in our previous study on ball grid array component rework [4]. During the pad redress step, most of the Pb-free solder left after component removal was consumed by using a Cu solder wick. The rest of the solder was heavily enriched with intermetallic particles. This remaining solder then mixed with the eutectic SnPb alloy used for rework. The excessive intermetallic particles caused a shift in SnPb solder composition from the near eutectic to off-eutectic.

Small intermetallic particles may also be precipitated during cooling from Sn and Pb based solid solutions. These particles were identified as Cu_6Sn_5. Although an extensive EDX analysis was performed, Ag was not found in reworked solder joints.

After 2X rework, the solder joint microstructure looks like that of a conventional SnPb interconnect - there are no large primary Cu_6Sn_5 crystals present in the solder joint (Figure 7)

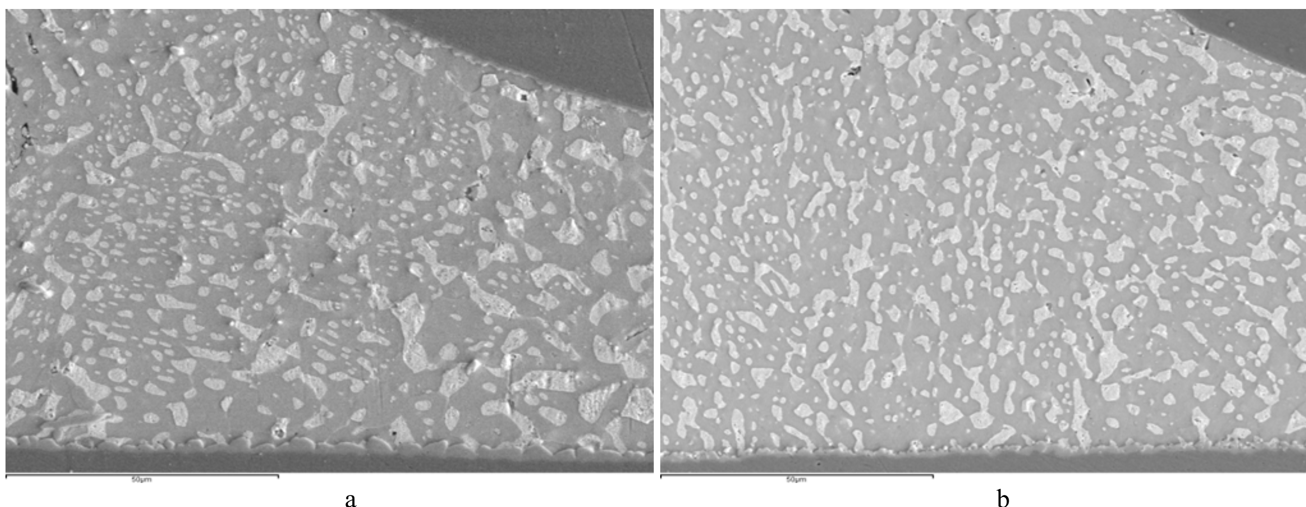

Figure 7: Typical microstructure of 2X reworked solder joints using SnPb solder, SEM, 1000X: a – TQFP-144; b – TSOP-50

The intermetallic layer formed between the Cu pads and solder in reworked SnPb joints was thinner than in SAC305 as-assembled joints (Figure 8). In the TSOP-50 and QFN-20 it was even thinner after 2X rework. Such a phenomenon was observed by the authors previously and may be explained by dissolution of the intermetallic layer in a fresh solder placed during rework. However, this thickness of intermetallic should not affect the quality or reliability of the solder joints.

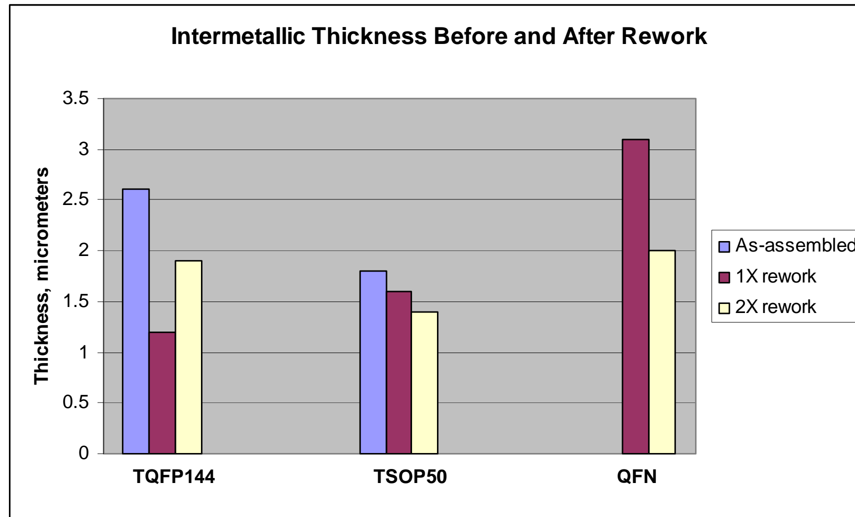

Figure 8: Intermetallic thickness before and after rework.

Drop Test Physical Failure Analysis

Pad cratering was the predominant failure mechanism in all components, as observed through both dye-and-pry and cross sectioning (Table 4 and Table 5). In two cases the cratering was significant enough to break the trace and cause an electrical failure, however in most cases the trace remained intact and therefore no electrical failure was detected. A small number of the analyzed solder joints had signs of solder fracture; however only in one case did this lead to an electrical failure. This indicates that, for the most part, the solder fractures did not penetrate through the entire solder joint.

Table 4: Dye and Pry Mechanical Failures

Board SN	Component						
	CLCC-20	QFN-20		TQFP-144			TSOP-50
60		U15**	U27*		U57*	U58	
81			U27**		U57*		U25*
82						U58*	
83					U57*	U58	U25*
84	U17**	U15**				U58*	
85		U15*		U3			
86			U27*		U57		U25**
87		U15*	U27**			U58	U25*

Green highlight indicates no failure
Red highlights indicate solder fracture
Orange highlights indicate pad cratering

** represents one rework performed*
*** represents two reworks performed*

Table 5: Cross-Sectioning Observations

Board SN	Component									
	CLCC-20	PDIP-20			QFN-20		TQFP-144			TSOP-50
60							U34**			
81					U15*					
82						U27*		U57		
83		U8**				U27**				
84	<u>U14</u>									U25**
85								<u>U57*</u>	U58	U25*
86		U8*	U30		<u>U15**</u>					
87				U38						

** represents one rework performed*
*** represents two reworks performed*
Components that are underlined represent electrical failure which occurred during the drop test

Green highlight indicates no failure
Red highlights indicate solder fracture
Orange highlights indicate pad cratering

Pad cratering occurred in all package types (CLCC-20, QFN-20, TQFP-144, TSOP-50) but was less prevalent in the TQFP-144 in which pad cratering was observed on only one out of nine dye-and-pry samples and was not at all found through cross sectioning. This is likely due to the structure of the part, which has compliant copper leads on all four sides, ensuring efficient stress distribution. However, in one part, the lead was found to fail through the solder in a fatigue failure mode (see Figure 9).

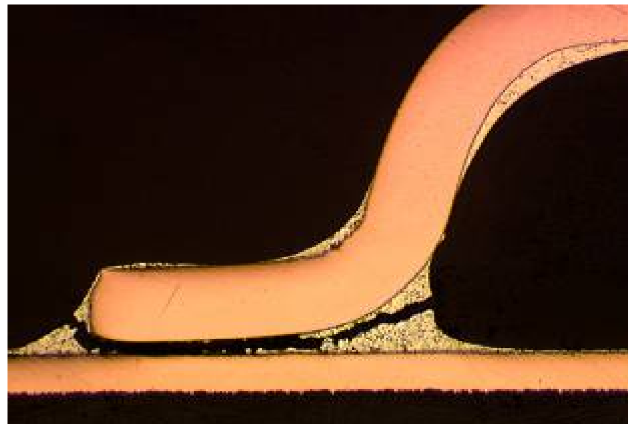

Figure 9: Fatigue failure of TQFP-144 with 1x rework as seen through cross sectioning

Partial solder joint cracks and pad cratering were both observed on the QFN-20 part, at approximately the same frequency. For example, in Figure 10, pin 1 of this QFN-20 package, shows some evidence of dye penetration through the bulk solder, indicating that a fracture was present prior to prying the component from the board. The penetration covers less then 25% of the solder surface near the top edge of the joint. Pin 2 shows almost complete dye penetration across the whole pin. The fracture appears to include the intermetallic surface.

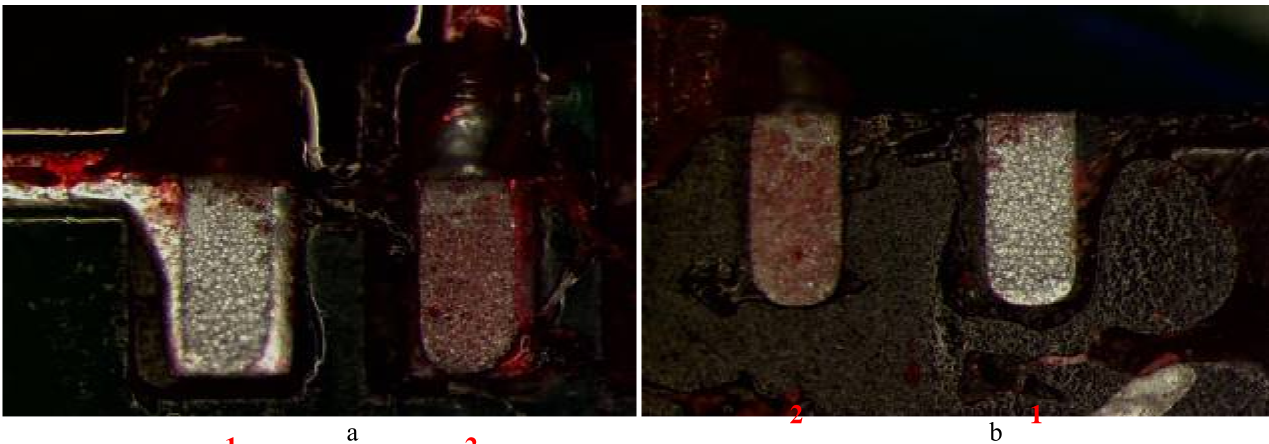

Figure 10: Dye and Pry results of a QFN-20 showing dye penetration through the bulk solder: a- board side; and b- component side

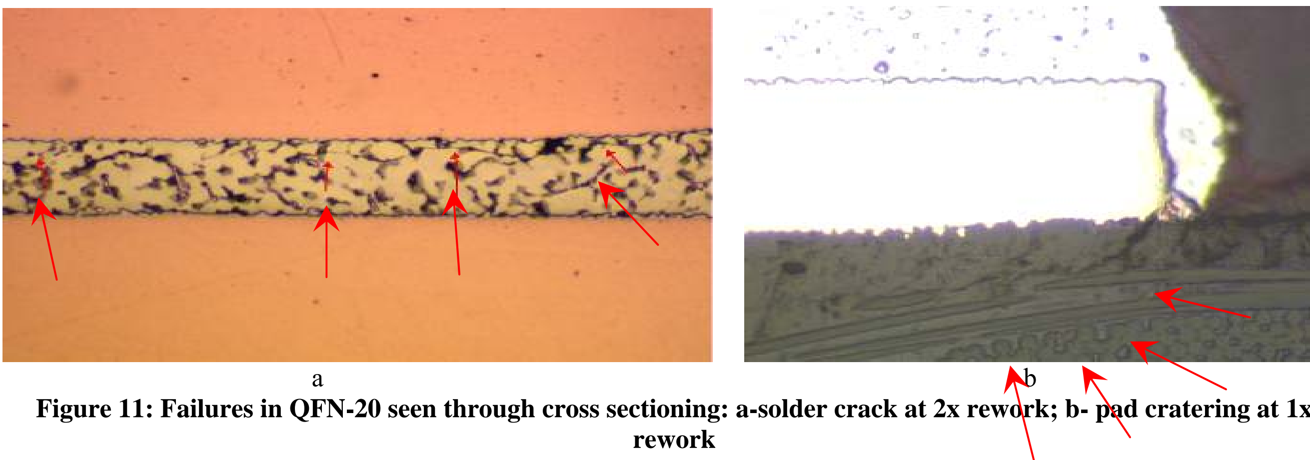

Figure 11: Failures in QFN-20 seen through cross sectioning: a-solder crack at 2x rework; b- pad cratering at 1x rework

Figure 11 shows cross sections which reveal both a fine crack through the bulk solder and pad cratering in a QFN-20 package.

Both the CLCC-20 parts tested and most of the TSOP-50 parts destructively analyzed show some degree of pad cratering. The cross section in Figure 12(a) illustrates an example of cratering that resulted in a broken trace which can explain the corresponding electrical failure. Figure 12(b) shows the typical pad cratering of a CLCC-20 viewed through dye-and-pry testing.

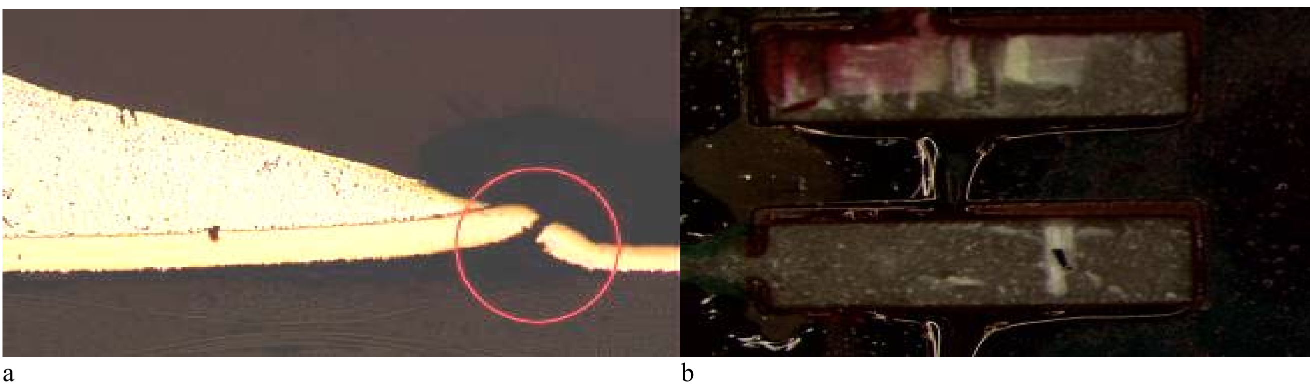

Figure 12: Pad cratering seen on CLCC-20 through: a- cross sectioning; b- dye-and-pry

In this analysis of 23 components, a total of three parts were found to have some mechanical damage in the solder, one of these resulted in an actual electrical failure. In all of these cases, the solder used was SnPb reworked, representing both mixed and SnPb solder. No solder damage were observed in the Pb-free, non-reworked components although the number of

samples that were subjected to physical failure analysis would be considered small. All mechanical failures in the Pb-free soldered components were the result of pad cratering. In this study only a small portion of the components were subjected to failure analysis. More of the components would need to be analyzed in order to increase confidence in the trends observed.

Conclusions

It was found that the predominant damage mechanism in drop testing is pad cratering. Cracks propagate through the board material between the laminate and glass fiber under the pads. Electrical failure was only observed when the Cu trace was completely broken. Of the leaded components that were electrically functional after drop testing, approximately one third were found to be mechanically damaged with pad cratering after dye-and-pry inspection. Whereas only three leaded components electrically failed (less than 1%): two were reworked and one was not reworked. Of those two reworked joints that failed, only the TQFP, the compliant leaded component, showed signs of SnPb solder joint fatigue fracture. The failure of the other two components was due to pad cratering. There was no correlation found between the number of reworks and the amount of electrical or mechanical failure since only three leaded components failed in the test. Most importantly, this sample set showed no difference in drop test performance between SnPb-reworked and non-reworked Pb-free solder joints for non-BGA components.

Since none of the BGAs were reworked in this study and the test resulted in only a small number of non-BGA electrical failures, the authors are unable to determine the comparative strength of Pb-free vs. SnPb-reworked samples other than to state that both survived the current test plan. Another important finding is that electrical testing is not enough to ascertain interconnect robustness during drop testing. Significant post-test destructive analysis is required to determine the level of mechanical damage.

Future Work

More data will be available upon completion of the NASA DoD Pb-free project including the failure analysis of the BGAs and results of vibration testing and thermal cycling performed on the same test vehicle with the same rework plan. Although it is out of the scope of the current mandate, drop testing on reworked BGAs should be performed to investigate any possible laminate degradation due to the multiple reflows. Future drop testing should employ a larger number of drops per board if the characterisitc failure life of the more compliant non-BGA components is required.

Acknowledgements

The Celestica authors would also like to acknowledge the support of fellow team members, Jie Qian and Zohreh Bagheri for their assistance with the failure analysis.

References

1. D. Suh, D.W. Kim, P. Liu, H. Kim, J.A. Weninger, C.M. Kumar, A. Prasad, B.W. Grimsley, and H.B. Tejada, “Effects of Ag content on fracture resistance of Sn-Ag-Cu lead-free solders under high-strain rate conditions,” *Materials Science and Engineering: A*, vol. 460-461, Jul. 2007, pp. 595-603.
2. J. Bragg, A. Lai and S. Subramaniam, “Strain Induced Assembly and Test Failures”, SMTA/CMAP International Conference on Soldering and Reliability, April 2007.
3. J. Bragg, J. Bookbinder, B. Harper and G. Sanders, “A Non-Destructive Visual Failure Analysis Technique for Cracked BGA Interconnects”, ECTC 2003 Conference Proceedings, pp. 886-890.
4. J. Bragg, “Pb-Free Failure Analysis Case Studies from an EMS Perspective”, SMTAI May 2008.
5. M. Kelly, M. Ferrill, P. Snugovsky, Z. Bagheri, R. Trivedi, G. Dinca and Chris Achong, “Rework Process Window and Microstructural Analysis for Lead-Free Mirrored BGA Design Points”, APEX Conf. (2009).